
Dynamic Relational Inference in Multi-Agent Trajectories

Ruichao Xiao

xiao.ruic@northeastern.edu
Northeastern University

Rose Yu

roseyu@northeastern.edu
Northeastern University, UC San Diego

Abstract

Inferring interactions from multi-agent trajectories has broad applications in physics, vision and robotics. Neural relational inference [26] (NRI) is a deep generative model that can reason about relations in complex dynamics without supervision. In this paper, we take a careful look at this approach for relational inference in multi-agent trajectories. First, we discover that NRI can be fundamentally limited without sufficient long-term observations. Its ability to accurately infer interactions degrades drastically for short output sequences. Next, we consider a more general setting of relational inference when interactions are changing over time. We propose an extension of NRI, which we call the DYnamic multi-Agent Relational Inference (DYARI) model that can reason about *dynamic* relations. We conduct exhaustive experiments to study the effect of model architecture, underlying dynamics and training scheme on the performance of dynamic relational inference using a simulated physics system. We also showcase the usage of our model on real-world multi-agent basketball trajectories.

1 Introduction

Particles, friends, teams, and alliances are multi-agent relations at different scales. Learning the relations among multiple agents deepens our understanding of the structures and dynamics underlying many systems. Practical examples include understanding social dynamics among pedestrians [1], learning communication protocols in traffic [42, 35] and predicting complex physical interactions of particles [36, 32, 38]. Graph neural networks (GNNs), e.g. [4, 16] are common deep learning frameworks for encoding relational information. However, GNNs assumes that the graph is given as *observed* relations. For multi-agent trajectories, the relations are typically *hidden* and thus need to be inferred from data. While one could impose a prior graph structure, it is difficult to find an appropriate one as the space of all structures is very large [14]. The search task is computationally expensive and the resulting model can potentially suffer from the model misspecification issue [28].

Relational inference aims to discover latent interaction structures from data and has been studied for decades in machine learning. Statistical relational learning are based on probabilistic graphical models such as probabilistic relational model [22, 11, 27, 40]. However, these methods may require significant feature engineering and high computational costs. Recently, [39] propose to reason about relations using neural networks but requires supervision. [26] propose Neural Relational Inference (NRI), a flexible deep generative model that can infer potential relations in an unsupervised fashion. NRI simultaneously learns the dynamics from multi-agent trajectories and infers their relations. In particular, NRI builds upon variational auto-encoder (VAE) [25] and introduces latent variables to represent the hidden relations. Despite its flexibility, NRI is still rather limited as it assumes the relations among the agents are *static* throughout the trajectories. Two agents are either interacting or not interacting regardless of their states at different time steps.

In this paper, we first ask the question: *whether neural relational inference is always possible?* Through exhaustive experiments using simulated dynamics physics systems, we discover that the performance of NRI is highly dependent on the length of the output sequence. Our findings highlight the importance of having sufficient temporal observations in decoding to infer the correct relations. Given these findings, we further investigate a more general setting, *dynamic* relational inference, where the relations among agents are time-varying. This lead to an extension of the NRI model, which we call DYnamic multi-Agent Relational Inference (DYARI). Our model is particularly suited to infer dynamic latent interactions that occurs in the real world. For example, in game play, agents can coordinate and compete in various ways depending on the strategy. In physics, moving particles can demonstrate weak or strong interactions depending on the distance.

We demonstrate our findings using a simulated physics dynamics system. We perform extensive experiments to validate the performance of dynamic relational inference with respect to model architecture, underlying dynamics and training schemes. We also showcase the usage of our DYARI model on real-world basketball trajectories. In summary, our contributions include:

- We discover pathological cases of neural relational inference [26] (NRI) which relate to the length of the output trajectories.
- We generalize static relational inference to dynamic setting and develop an extension of NRI to handle time-varying interactions.
- We demonstrate the effectiveness our method on both the simulated physics dynamics and real-world basketball game play datasets.

2 Related work

Deep sequence models The rise of deep learning has led to development in both deterministic sequence models [47, 1, 44, 31] and stochastic sequence models [9, 10, 29, 37, 8, 19, 48]. For stochastic models, there are roughly three types of framework: GAN [12], VAE [25], and normalizing flow [24]. GAN-like models, [48] combine adversarial training and a supervised learning objective for time series forecasting. [34] propose a non-autoregressive model for sequence generation. Compared with GAN, VAE-type models can provide explicit inference and are preferable for our purpose. For instance, [9] introduces stochastic layers in recurrent neural networks to model speech and hand-writing. [37] parameterizes a linear state-space model for probabilistic time series forecasting. [8, 19] combine normalizing flows with autoregressive models. However, all existing stochastic sequence models can only infer the *temporal* latent states for individual sequence rather than the *relations* among them.

Relational inference Interaction-based networks or graph networks (GNs) seek to learn representations over relational data, see several recent surveys on GNs and the references therein [7, 49, 46, 13]. Unfortunately, most existing work assume the graph structure is observed while relational inference aims to discover the latent interactions from data. For relational reasoning, earlier work [22, 11, 27] uses probabilistic graphical model to infer the relations, but requires significant feature engineering and the inference is computationally intensive. [39] propose to use neural networks to reason in dynamic physical system but their model requires supervision signals. The seminal work of NRI performs unsupervised learning for relational inference where the graph structure is estimated from trajectories. [3] reformulates the problem in NRI as meta-learning and proposes simulated annealing to search for graph structures. However, both [26] and [3] are limited to *static* relations whereas our innovation is mainly on the *dynamic* relations.

Multi-agent learning Multi-agent trajectories arises frequently in reinforcement learning (RL) and imitation learning (IL) [33, 2, 20]. Modeling agent interactions given dynamic observations from the environment remains a central topic. In the RL setting, for example, [42] models the control policy in a fully cooperative multi-agent setting and applies a GN to represent the communications. [30] models the agents coordination as a latent variable for imitation learning. [41] generalizes generative adversarial imitation learning [18] to multi-agent setting through a shared generator. However, these coordination models only capture the global interactions implicitly without the explicit graph structure. [43] combines GN with a forward dynamics model to model multi-agent coordination but also requires supervised training. [15] directly models the episodes of interaction data with GNNs for learning multi-agent policies. Our method instantiates the multi-agent imitation learning framework, but focuses on *unsupervised* reasoning about relations from trajectories. Our approach is also applicable to dynamic modeling in model-based RL.

3 Dynamic Multi-Agent Relational Inference

Given a collection of multi-agent trajectories, we aim to reason about their hidden relations given information only about their dynamics. First we describe the multi-agent relational inference problem in its most general form. Then we consider unsupervised learning with deep generative models.

3.1 Probabilistic inference formulation

We formally describe the relational inference problem using the language of Markov games [33]. Consider a total of N agents $i \in \{1, \dots, N\}$, each of which has a separate state space $\mathcal{S}^{(i)}$ and action space $\mathcal{A}^{(i)}$. A policy $\pi^{(i)}$ represents a mapping from states to actions: $\pi^{(i)} : \mathcal{S} \rightarrow \mathcal{A}$. At every time step t , an agent executes an action $a_t^{(i)} \in \mathcal{A}^{(i)}$ at state $s_t^{(i)} \in \mathcal{S}^{(i)}$ according to its policy. A trajectory $\tau = (x_1, x_2, \dots, x_T)$ is thus a sequence of state-action pairs that is sampled from such a stochastic policy, where $x_t = (s_t, a_t)$.

Given a collection of multi-agent trajectories $\{\tau^{(i)}\}_{i=1}^N$, we aim to infer the pairwise interactions at every time step. We can interpret the interaction as cooperative or competitive relations that can be highly dynamic. The joint distribution of multi-agent trajectories under the policy $\pi := \{\pi^{(i)}\}_{i=1}^N$ can be written as:

$$p_\pi(\tau^{(1)}, \dots, \tau^{(N)}) = \prod_{t=1}^T p(\mathbf{x}_{t+1} | \mathbf{x}_t, \dots, \mathbf{x}_1) \quad (1)$$

where $p(\mathbf{x}_{t+1} | \mathbf{x}_t, \dots, \mathbf{x}_1)$ represents the underlying dynamics and the policy. We use the bold form $\mathbf{x}_t := (x_t^{(1)}, \dots, x_t^{(N)})$ to denote the concatenation of all agents observations.

In relational inference, we introduce latent variables $z_t^{(ij)}$ to denote the interactions between agent i and j at time t . To make the problem tractable, we restrict $z_t^{(ij)}$ to be categorical, representing discrete interactions such as coordination or competition. We assume the dynamics model can be decomposed into the individual dynamics, in conjunction with the pairwise interaction. This substantially reduces the dimensionality of the distribution and simplifies learning. Therefore, we can rewrite the transition probability as:

$$p(\mathbf{x}_{t+1} | \mathbf{x}_t, \dots, \mathbf{x}_1) \approx \int_{\mathbf{z}} \prod_{i=1}^N p(x_{t+1}^{(i)} | x_t^{(i)}) \prod_{i=1}^N \prod_{j=1, j \neq i}^N p(z_t^{(ij)} | x_t^{(i)}, x_t^{(j)}) d\mathbf{z} \quad (2)$$

Here each $p(x_{t+1}^{(i)} | x_t^{(i)})$ captures the dynamics of individual agent. The distribution $p(z_t^{(ij)} | x_t^{(i)}, x_t^{(j)})$ expresses the latent relations between a pair of agents. Figure 1 visualizes the graphical model representation for three agents. The shaded nodes represent observed variables and the unshaded nodes are latent variables.

3.2 Neural relational inference

In Neural Relational Inference (NRI) [26], the relations are assumed to be static, that is $z_1^{(ij)} \dots = z_t^{(ij)}$ for all time steps t . NRI uses a variational auto-encoder (VAE) framework with a GNN encoder and decoder. The encoder is a graph neural network that takes an embedding of multi-agent trajectories and encodes them into hidden representations. For each pair of agents, the encoder generates a distribution over possible relations, which are then reparametrized using the Gumbel softmax to obtain the interaction graph. The decoder propagates the hidden representations given the interaction graph to generate future predictions in an auto-regressive fashion.

Pathological cases of NRI It is known that latent variable models suffer from the problem of identifiability [28], which means certain parameters, in principle, cannot be estimated consistently. Even though identification is not statistical inference in a strict sense, it can cause difficulty in learning the correct relations. Therefore, we question the learning setup of NRI and ask: *whether neural relational inference is always possible*.

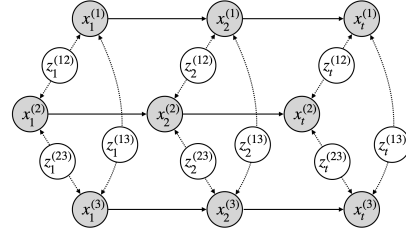


Figure 1: Probabilistic graphical model representation of dynamic multi-agent relational inference. Shaded nodes are observed and unshaded nodes are latent variables.

To answer this question, we use the interacting particles simulation in NRI. As shown in Figure 2, given trajectories of 5 particles connected by springs, we aim to learn the dynamics and interactions by inferring the underlying interaction graph. As the interactions are known (springs), we report the accuracy of unsupervised interaction discovery compare with ground truth. All the experiments follow the exact same setting as NRI and the decoder is trained using teacher forcing [45]. Note that the target interaction graph here is static.

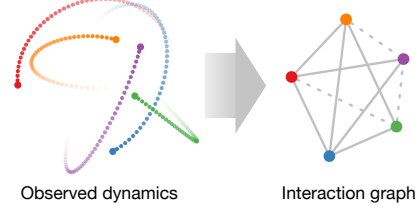


Figure 2: Inferring interaction graph from trajectories with neural relational inference. Picture taken from [26]

We evaluate the relational inference performance of NRI in a variety of scenarios by varying the length of input and output trajectories. Specifically, each sample sequence consists of trajectories from 5 particles of 50 time steps. Table 1 summarizes the unsupervised relational inference accuracy with different combination of trajectory length in encoder and decoder. We can see that the inference accuracy decreases significantly with shorter outputs. This phenomena is consistent across different input lengths. For relational inference with 40 time step encoding and 10 step decoding, the accuracy drops to as low as 53%, which signals that NRI is incapable of learning the interaction graph correctly.

Table 1: Inference accuracy (%) of NRI trained with different input/output trajectory lengths. Note that the performance deteriorates significantly when the output length decreases.

Input length	Output Trajectory length				
	10	20	30	40	50
40	53.4 ± 0.4	64.2 ± 0.2	83.5 ± 0.1	98.4 ± 0.1	99.9 ± 0.0
50	54.2 ± 0.3	66.8 ± 0.5	85.6 ± 0.1	98.6 ± 0.0	99.9 ± 0.0

The pathological cases for NRI highlight the importance of having long output sequences for relational inference: *without sufficient time steps in the output sequences to decode, NRI can fail miserably.* This phenomena poses a great barrier to more general dynamic relational inference. In particular, we consider the scenario where the interaction can appear and disappear. An edge may change in the interaction graph only after a short period of time. There may not exist long enough output sequences to properly learn the interactions. With this in mind, we describe our extension of the NRI model to the dynamic relational inference problem.

3.3 Dynamic Multiagent Relational Inference (DYARI)

NRI assumes the interaction graph is static, which is rather restrictive for practical applications. We propose Dynamic multi-Agent Relational Inference (DYARI), to capture dynamic relations.

Generation model Given the latent interaction variables, the generative model assumes the prediction at each time step follows a Gaussian distribution:

$$p(x_{t+1}^{(i)} | z_t^{(ij)}) = \mathcal{N}(x_{t+1}^{(i)} | h_{t+1}^{(i)}, \sigma_x^2 I) \quad (3)$$

$$h_{t+1}^i = f_{\text{gnn+rnn}}(\sum_{j \neq i} \sum_k z_t^{(ij)}(k) u(k); \theta), \quad u(k) = f_{\text{mlp}}^k(h_t^{(ij)}) \quad (4)$$

where $x_{t+1}^{(i)}$ is reparameterized using a Gaussian distribution with mean $h_{t+1}^{(i)}$ and standard deviation σ_x^2 . The hidden states $h_{t+1}^{(i)}$ of agent i is computed by aggregating the hidden states of all other agents. The latent variable $z_t^{(ij)}$ is categorical where we use the index k to indicate the k -th binary entry. To generate long-term predictions using the model in Eqn. (4), we can also incorporate the predictions from the previous time step: $h_{t+1}^i = f_{\text{dec}}(\sum_{j \neq i} z_t^{(ij)} h_t^{(ij)}, x_t^i; \theta)$

Inference model We assume discrete interactions such as coordination or competition, hence $z_t^{(ij)}$ follows a categorical distribution. Using the standard formulation of VAE, we can write down the inference model as follows:

$$q_\phi(z_t^{(ij)} | x_t^{(i)}, x_t^{(j)}) = \text{Cat}(h_t^{ij}), \quad h_t^{(ij)} = f_{\text{enc}}(h_t^{(i)}, h_t^{(j)}; \phi) \quad (5)$$

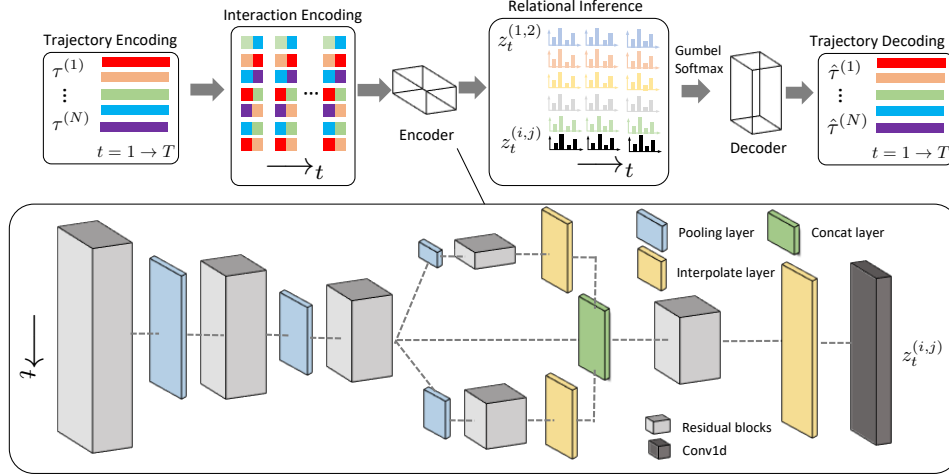


Figure 3: Visualization of the DYARI model. It infers pairwise relations at different time steps given trajectories. The bottom diagram shows the details of the encoder and the decoder is the same as NRI.

where $\text{Cat}(\cdot)$ is the categorical distribution. Using the Gumbel-Max trick [21], we can reparameterize the categorical distribution as: $z_t^{(ij)} = \text{Softmax}(h_t^{(ij)} + g_t^{(ij)})$. Here $h_t^{(ij)}$ is the mean vector of the interactions and $g_t^{(ij)}$ is a random Gumbel vector. The encoder f_{enc} infer the interactions based on the hidden states. To model the dynamics, we assume the hidden states of agent i at the next time step $h_{t+1}^{(i)}$ is a function of the interactions from all the other agents. The hidden states are propagated using the following equations:

$$h_t^{(i)} = f_{\text{gnn}}\left(\sum_{j \neq i} h_t^{(ij)}, x_t^{(i)}\right), \quad h_t^{(j)} = f_{\text{gnn}}\left(\sum_{i \neq j} h_t^{(ij)}, x_t^{(j)}\right), \quad f_{\text{cnn}}(h_1^{(i)}, \dots, h_t^{(i)}) \quad (6)$$

This is analogous to message passing in a graph where the node state is updated as an aggregation of messages from its neighbours. Note that a key difference between the model in Eqn. (4) and (5) and NRI is that the latent variable $z_t^{(ij)}$ is time-dependent, capturing dynamic interactions. We can train the generative model by maximizing the ELBO.

Model architecture We use the same decoder architecture as in NRI. For encoder, we propose several modifications to make it compatible with dynamic relation inference. Specifically, we adopt a temporal CNN architecture as it is well suited to extract rich dynamic features from sub-sequences, which is crucial for our task. Figure 3 visualizes the overall pipeline of our model which encodes multi-agent trajectories into interactions encoding. Based on the interactions encoding, the model infers the dynamic relations and reconstructs the sequences as a decoding process. The bottom cut-out diagram shows the architecture of our modified encoder. In particular, we use an architecture similar to ResNet [17] to increase its expressive capacity. The encoder of DYARI consists of several residual blocks to extract sub-sequences representations at multiple resolutions, and we use interpolation layers to reshape the hidden representations to the desired prediction length.

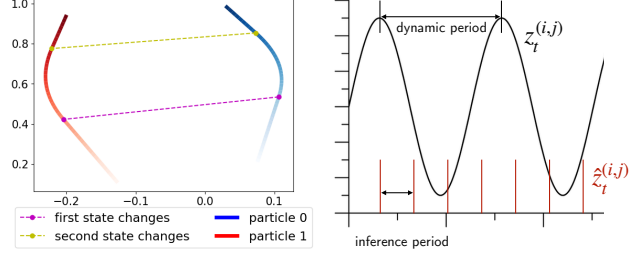
4 Experiments

In this section, we conduct extensive experiments on the simulated physics system to validate the performance of our method. We further apply the DYARI model to a real-world competitive basketball trajectory dataset for unsupervised learning of hidden interactions.

4.1 Physics Simulations

The majority of our experiments is conducted using the simulation environment of particles connected by springs (Spring) Dataset [26]. This is ideal for model verification and ablative study because the ground truth interactions are known. By working with various simulation settings, we can diagnose the complexity of the dynamical system and obtain quantitative measures for model performance.

Dataset Generation Specifically, the Spring dataset simulates movements of a group of particles in a box. A spring connects each pair of particles with certain probability. Formally, let $z_t^{(i,j)}$ be the binary random variable which indicates whether there is a spring between particle i, j at time t .



To simulate the dynamic inference setting, we generate the trajectories using $z_t^{(i,j)}$ that changes over time. To simplify the problem, we assume the change to be periodic and define the number of time steps between the change of interactions as **dynamic period**, denoted by a . For binary interactions, we have $z_{t+a}^{(i,j)} = -z_t^{(i,j)}$. The smaller the dynamic period is, the more dynamic the system interactions become, hence more difficult to perform inference. Figure 4 left plot visualizes sample trajectories of two particles with a spring appears and disappears. Notice that the two particle trajectories start as straight lines and bend in the middle due to the force of the spring, and go back to straight lines after the removal of the spring.

Figure 4: Left: example trajectories of two particles. There are two state changes in the example (corresponding to $0 \rightarrow 1 \rightarrow 0$). The trajectories start from the end with lighter color and gradually become darker. Right: visualization of dynamic period in black and inference period in red.

Experimental Setup We simulate 5 particles trajectories with 50k training sequence, 10k validation and testing sequences, each of length 40. At every time step t , we infer a different $z_t^{(i,j)}$ to capture the dynamic relations among particles using our proposed encoder architecture. We assume $p_\theta(\mathbf{z})$ to be a uniform distribution and use ELBO as the optimization objective:

$$\begin{aligned} \mathcal{L}_{\text{ELBO}} &= \mathbb{E}[\log p_\theta(\mathbf{x}|\mathbf{z})] - \beta d_{\text{KL}}[q_\phi(\mathbf{z}|\mathbf{x})||p_\theta(\mathbf{z})]] \\ &= -\sum_i \sum_{t=1}^T \frac{(\hat{\mu}_t^i - x_t^i)^2}{2\sigma^2} + \beta \sum_{i,j} \sum_{t=1}^T H(q_\phi(z_t^{(i,j)}|\mathbf{x})) + \text{constant} \end{aligned} \quad (7)$$

where β is applied to control the scale of two parts of the losses. Unless noted explicitly, all the models are trained using the Adam [23] optimizer with learning rate 0.0005, weight decay 0.0001 for 300 epochs by default.

In practice, we do not know the dynamic period of the trajectories beforehand. Therefore, how often we infer the interactions reflects our inductive bias of the relational dynamics: rare predictions would miss the interaction changes while predicting too frequently could introduce more latent variables and complicate the inference. To investigate this trade-off, we define **inference period** for the number of time steps between two predictions $\hat{z}_t^{(i,j)}$, as shown in Figure 4 right plot.

4.1.1 Inference model architecture comparison

We compare the performance of different model architectures. NRI is designed to infer a static graph, and we use DYARI to perform dynamic relational inference. We compare two variations of our model: DYARI-S for the simple model and DYARI-C for a more complex architecture. DYARI-C has more skip connections in the residual blocks, which also means it has around twice as many parameters as DYARI-S. All the models are trained to predict the sequence in an auto-regressive fashion: the prediction of current time step is fed as the input to the next time step.

We first vary the dynamic period from 40 to 5 to simulate different dynamics with increasing frequency. The inference period is set to be the same as the dynamic period. All decoding sequences are of length 40. The quantitative results of trajectory prediction mean square error (MSE) and interaction inference accuracy are presented in the Table. 2.

We can see that all methods can achieve almost perfect reconstruction of the trajectories with very low MSE. However, NRI is incapable of learning dynamic interactions while ours succeeds. By increasing the model capacity, DYARI is able to reach higher accuracy. Thus one of effective way to learn the dynamic relations is to increase model capacity. However, when the dynamic period is small (5), increasing model capacity does not help with the dynamic relational inference even with very small

Table 2: Qualitative results for different encoder. Accuracy improves by increasing the model capacity. In the training, The inference period of the two DYARI match with the dynamic period.

Dynamic Period	MSE				Accuracy			
	40(static)	20	10	5	40(static)	20	10	5
NRI(learned)	2.7e-5	9.2e-5	5.9e-5	2.5e-6	0.99	0.51	0.50	0.50
DYARI-S	2.6e-5	7.3e-5	5.7e-5	2.6e-6	0.99	0.83	0.55	0.51
DYARI-C	2.6e-5	4.1e-5	1.2e-5	2.1e-6	0.99	0.92	0.87	0.53

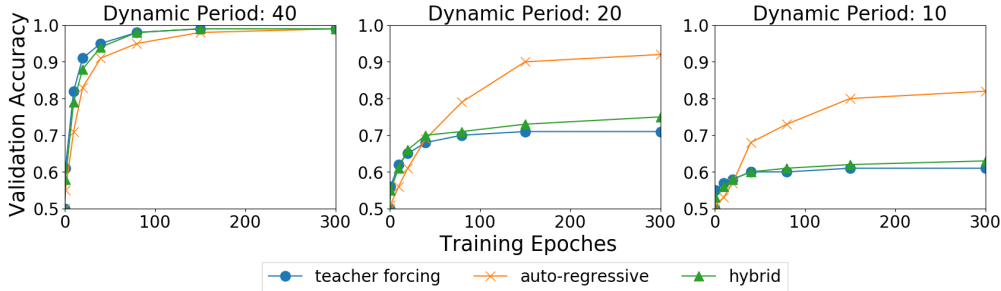


Figure 5: Sampled learning curve of DYARI-C for different learning schemes in decoder. The inference period matches the dynamic period for the training. hybrid scheme refers to train with teacher forcing at the beginning 30 time steps and auto-regressive in the later 10 time steps.

reconstruction error. It suggests that neural relational inference methods are still limited in learning the correct interactions with frequent changes in the dynamics.

4.1.2 Trade-off in dynamic and inference period

There exists a nuanced trade-off between dynamics period and inference period: rare predictions would miss the interaction changes (low accuracy) while predicting too frequently could introduce more latent variables (high stochasticity). To demonstrate this trade-off, we repeat the experiments by varying both the dynamic period and inference period from 40 to 5 time steps.

In Table 3, we observe that dynamic relational inference reaches the highest accuracy when the inference period perfectly matches the dynamic period. However, if the inference period is smaller than the dynamic period, the model fails to learn the correct hidden relations. If the inference period is larger than the dynamic period, the model is still able to make reasonable predictions but suffers from low accuracy.

Table 3: Inference accuracy for different dynamic periods and inference periods with DYARI-C. When the inference period matches the dynamic period, the relation inference accuracy is the best.

Dynamic Period		40	20	10	5
Inference Period	40(static)	0.99	0.50	0.50	0.50
	20	0.95	0.92	0.50	0.50
	10	0.62	0.70	0.87	0.50
	5	0.58	0.60	0.55	0.53

We identify three key observations for dynamic relational inference (1) When the dynamic period decreases, the system dynamics become more complex and hence the performance deteriorates; (2) To obtain the best performances, it is desirable to have matching periods for the underlying dynamics and the inference algorithm. But this is difficulty as the dynamic period is unknown in most cases; (3) Simply decreasing the inference period is also not enough. When the inference period is very small, the stochasticity introduced by the inference task also affects the predictions.

4.1.3 Decoder training scheme

A fundamental challenge in sequence prediction is covariate shift [6] – a mismatch between distribution in training and testing – due to sequential dependency. Common solutions to mitigate covariate shift include teacher forcing [45] and scheduled sampling [5]. However, all these work are focused the prediction of *observed* sequence while our sequence predictions are on the *latent* variables. It is not evident that covariate shift exists in this setting. We demonstrate the empirical evidence for the effect of different training schemes on the accuracy of relational inference.

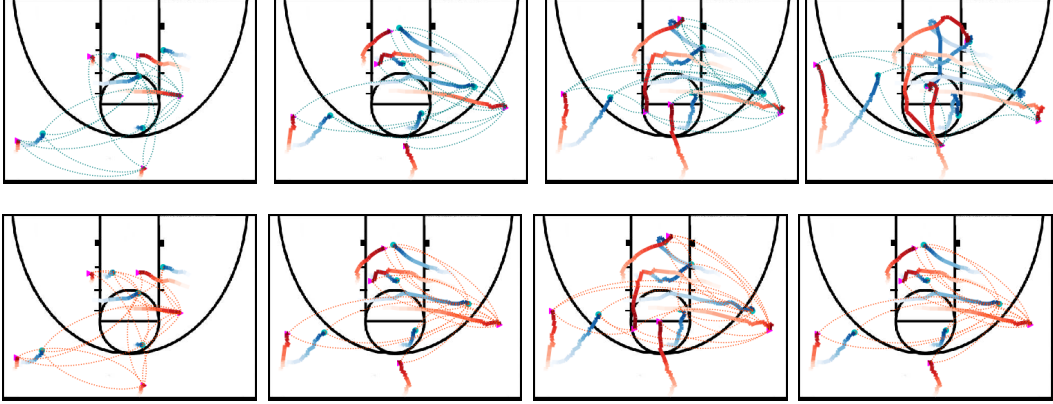


Figure 6: Visualization of the basketball players trajectories with inference period = 10. The top row visualizes the inferred dynamic interactions from the same team (coordination) and the bottom row visualizes the inferred interactions from different teams (competition). Different columns represent different time steps. (Additional inferred relations visualized in the Appendix.)

We found that one significant factor that affects dynamic relations learning is using teacher forcing. Figure. 5 summarizes the difference in learning curve between using teacher forcing and auto-regressive for different dynamic periods. We also include a combined scheme (hybrid): the first 30 time-steps are trained with teacher forcing and then auto-regressive is used in the last 10 time-steps. We observe that while teacher forcing converges faster, it also leads to lower accuracy. Such an observation is consistent across different dynamic periods.

4.2 Real-World Basketball Data Experiments

We apply DYARI to a real world basketball trajectory dataset. The basketball dataset contains trajectories for 10 players in a game, which include 50,000 training samples, 10,000 validations samples and 10,000 test samples. Since the ground-truth of the interactions are unknown, we report the MSE loss and negative ELBO as in-direct measures for the relational inference performance. We set the number of interaction types to be 2 to represent coordination and competition. All the data are normalized into range $[0, 1]$ and trained with auto-regressive. The model is trained with batch size 64 and the same training strategy used in the physics simulation experiments.

MSE and negative ELBO values are reported in Table. 4. With smaller inference period, we observe lower MSE loss and negative ELBO. Intuitively, the interactions in the real world may change constantly, thus it would be helpful to use smaller inference period to model such dynamics. Fig. 7 visualizes a sample trajectory of 10 basketball players with inferred relations from DYARI-C over different time steps. We separate coordination and competition interactions in different rows. We can see clear attentions drawn to specific players through out the play.

Inference Period		40	20	10	5
MSE	NRI	2.3e-3	-	-	-
	DYARI-S	2.1e-3	1.3e-3	8.9e-4	7.8e-4
	DYARI-C	2.2e-3	8.4e-4	7.5e-4	6.4e-4
NELBO	NRI	13.71	-	-	-
	DYARI-S	11.98	8.21	7.02	4.77
	DYARI-C	12.65	6.16	4.38	3.67

Table 4: MSE loss and negative ELBO on basketball dataset. All the models are trained with auto-regressive.

5 Conclusion

We investigate neural relational inference (NRI) for unsupervised learning of dynamic interaction in multi-agent trajectories. We discover pathological cases where NRI can fail when the trajectories do not have enough length to decode. We further generalize NRI to infer *dynamic* interactions, leading to a novel deep generative model: Dynamic multi-Agent Relational Inference (DYARI). We perform extensive experiments to study the performance of DYARI in handling dynamic relations. We demonstrate the effectiveness of our model using simulated physics systems and a real-world multi-agent basketball trajectories dataset.

Broader Impact

Coordination, cooperation and competition are ubiquitous in both the physical and natural human world. From a group of interacting particles to a team of basketball players coordinating in a game, the scale and scope of multi-agent relations is fundamental to the structures and dynamics of a wide range of systems. However, reasoning about the hidden multi-agent relations given observations only from their motion is a fundamental challenge for multi-agent learning. At the core of this challenge is the inherent ambiguity of the relations as they are often dynamic. Our research cuts into the core of multi-agent learning, unfolding the limitations of existing neural inference solutions, and generalizing to capture dynamic relations. Our research shed lights on the socially aware AI systems to learn the cooperation patterns of human partners. The potential risk is the mis-use of our technology for disruptive military purposes to infer enemy and alliances relations.

References

- [1] A. Alahi, K. Goel, V. Ramanathan, A. Robicquet, L. Fei-Fei, and S. Savarese. Social lstm: Human trajectory prediction in crowded spaces. In *Proceedings of the IEEE conference on computer vision and pattern recognition*, pages 961–971, 2016.
- [2] S. V. Albrecht and P. Stone. Autonomous agents modelling other agents: A comprehensive survey and open problems. *Artificial Intelligence*, 258:66–95, 2018.
- [3] F. Alet, E. Weng, T. Lozano-Pérez, and L. P. Kaelbling. Neural relational inference with fast modular meta-learning. In *Advances in Neural Information Processing Systems*, pages 11804–11815, 2019.
- [4] P. Battaglia, R. Pascanu, M. Lai, D. J. Rezende, et al. Interaction networks for learning about objects, relations and physics. In *Advances in neural information processing systems*, pages 4502–4510, 2016.
- [5] S. Bengio, O. Vinyals, N. Jaitly, and N. Shazeer. Scheduled sampling for sequence prediction with recurrent neural networks. In *Advances in Neural Information Processing Systems*, pages 1171–1179, 2015.
- [6] S. Bickel, M. Brückner, and T. Scheffer. Discriminative learning under covariate shift. *Journal of Machine Learning Research*, 10(Sep):2137–2155, 2009.
- [7] M. M. Bronstein, J. Bruna, Y. LeCun, A. Szlam, and P. Vandergheynst. Geometric deep learning: going beyond euclidean data. *IEEE Signal Processing Magazine*, 34(4):18–42, 2017.
- [8] T. Q. Chen, Y. Rubanova, J. Bettencourt, and D. K. Duvenaud. Neural ordinary differential equations. In *Advances in neural information processing systems*, pages 6571–6583, 2018.
- [9] J. Chung, K. Kastner, L. Dinh, K. Goel, A. C. Courville, and Y. Bengio. A recurrent latent variable model for sequential data. In *Advances in neural information processing systems*, pages 2980–2988, 2015.
- [10] M. Fraccaro, S. K. Sønderby, U. Paquet, and O. Winther. Sequential neural models with stochastic layers. In *Advances in neural information processing systems*, pages 2199–2207, 2016.
- [11] L. Getoor, N. Friedman, D. Koller, and A. Pfeffer. Learning probabilistic relational models. In *Relational data mining*, pages 307–335. Springer, 2001.
- [12] I. Goodfellow, J. Pouget-Abadie, M. Mirza, B. Xu, D. Warde-Farley, S. Ozair, A. Courville, and Y. Bengio. Generative adversarial nets. In *Advances in neural information processing systems*, pages 2672–2680, 2014.
- [13] P. Goyal and E. Ferrara. Graph embedding techniques, applications, and performance: A survey. *Knowledge-Based Systems*, 151:78–94, 2018.
- [14] R. Grosse, R. R. Salakhutdinov, W. T. Freeman, and J. B. Tenenbaum. Exploiting compositionality to explore a large space of model structures. *arXiv preprint arXiv:1210.4856*, 2012.
- [15] A. Grover, M. Al-Shedivat, J. K. Gupta, Y. Burda, and H. Edwards. Learning policy representations in multiagent systems. *Proceedings of the 35th International Conference on Machine Learning*, 2018.
- [16] W. Hamilton, Z. Ying, and J. Leskovec. Inductive representation learning on large graphs. In *Advances in neural information processing systems*, pages 1024–1034, 2017.
- [17] K. He, X. Zhang, S. Ren, and J. Sun. Deep residual learning for image recognition. In *Proceedings of the IEEE conference on computer vision and pattern recognition*, pages 770–778, 2016.
- [18] J. Ho and S. Ermon. Generative adversarial imitation learning. In *Advances in neural information processing systems*, pages 4565–4573, 2016.
- [19] C.-W. Huang, D. Krueger, A. Lacoste, and A. Courville. Neural autoregressive flows. In *International Conference on Machine Learning*, pages 2078–2087, 2018.
- [20] M. Jaderberg, W. M. Czarnecki, I. Dunning, L. Marris, G. Lever, A. G. Castaneda, C. Beattie, N. C. Rabinowitz, A. S. Morcos, A. Ruderman, et al. Human-level performance in 3d multiplayer games with population-based reinforcement learning. *Science*, 364(6443):859–865, 2019.
- [21] E. Jang, S. Gu, and B. Poole. Categorical reparametrization with gumbel-softmax. In *International Conference on Learning Representations (ICLR 2017)*. OpenReview. net, 2017.
- [22] C. Kemp and J. B. Tenenbaum. The discovery of structural form. *Proceedings of the National Academy of Sciences*, 105(31):10687–10692, 2008.

- [23] D. P. Kingma and J. Ba. Adam: A method for stochastic optimization. *arXiv preprint arXiv:1412.6980*, 2014.
- [24] D. P. Kingma, T. Salimans, R. Jozefowicz, X. Chen, I. Sutskever, and M. Welling. Improved variational inference with inverse autoregressive flow. In *Advances in neural information processing systems*, pages 4743–4751, 2016.
- [25] D. P. Kingma and M. Welling. Auto-encoding variational bayes. *arXiv preprint arXiv:1312.6114*, 2013.
- [26] T. Kipf, E. Fetaya, K.-C. Wang, M. Welling, and R. Zemel. Neural relational inference for interacting systems. In *International Conference on Machine Learning*, pages 2688–2697, 2018.
- [27] D. Koller, N. Friedman, S. Džeroski, C. Sutton, A. McCallum, A. Pfeffer, P. Abbeel, M.-F. Wong, D. Heckerman, C. Meek, et al. *Introduction to statistical relational learning*. MIT press, 2007.
- [28] T. C. Koopmans and O. Reiersol. The identification of structural characteristics. *The Annals of Mathematical Statistics*, 21(2):165–181, 1950.
- [29] R. G. Krishnan, U. Shalit, and D. Sontag. Structured inference networks for nonlinear state space models. In *Thirty-first aaaa conference on artificial intelligence*, 2017.
- [30] H. M. Le, Y. Yue, P. Carr, and P. Lucey. Coordinated multi-agent imitation learning. In *Proceedings of the 34th International Conference on Machine Learning-Volume 70*, pages 1995–2003. JMLR. org, 2017.
- [31] S. Li, X. Jin, Y. Xuan, X. Zhou, W. Chen, Y.-X. Wang, and X. Yan. Enhancing the locality and breaking the memory bottleneck of transformer on time series forecasting. In *Advances in Neural Information Processing Systems*, pages 5244–5254, 2019.
- [32] Y. Li, J. Wu, R. Tedrake, J. B. Tenenbaum, and A. Torralba. Learning particle dynamics for manipulating rigid bodies, deformable objects, and fluids. *arXiv preprint arXiv:1810.01566*, 2018.
- [33] M. L. Littman. Markov games as a framework for multi-agent reinforcement learning. In *Machine learning proceedings 1994*, pages 157–163. Elsevier, 1994.
- [34] Y. Liu, R. Yu, S. Zheng, E. Zhan, and Y. Yue. Naomi: Non-autoregressive multiresolution sequence imputation. In *Advances in Neural Information Processing Systems*, pages 11236–11246, 2019.
- [35] R. Lowe, Y. I. Wu, A. Tamar, J. Harb, O. P. Abbeel, and I. Mordatch. Multi-agent actor-critic for mixed cooperative-competitive environments. In *Advances in neural information processing systems*, pages 6379–6390, 2017.
- [36] D. Mrowca, C. Zhuang, E. Wang, N. Haber, L. F. Fei-Fei, J. Tenenbaum, and D. L. Yamins. Flexible neural representation for physics prediction. In *Advances in neural information processing systems*, pages 8799–8810, 2018.
- [37] S. S. Rangapuram, M. W. Seeger, J. Gasthaus, L. Stella, Y. Wang, and T. Januschowski. Deep state space models for time series forecasting. In *Advances in neural information processing systems*, pages 7785–7794, 2018.
- [38] A. Sanchez-Gonzalez, J. Godwin, T. Pfaff, R. Ying, J. Leskovec, and P. W. Battaglia. Learning to simulate complex physics with graph networks. *arXiv preprint arXiv:2002.09405*, 2020.
- [39] A. Santoro, D. Raposo, D. G. Barrett, M. Malinowski, R. Pascanu, P. Battaglia, and T. Lillicrap. A simple neural network module for relational reasoning. In *Advances in neural information processing systems*, pages 4967–4976, 2017.
- [40] M. Shum, M. Kleiman-Weiner, M. L. Littman, and J. B. Tenenbaum. Theory of minds: Understanding behavior in groups through inverse planning. In *Proceedings of the AAAI Conference on Artificial Intelligence*, volume 33, pages 6163–6170, 2019.
- [41] J. Song, H. Ren, D. Sadigh, and S. Ermon. Multi-agent generative adversarial imitation learning. In *Advances in neural information processing systems*, pages 7461–7472, 2018.
- [42] S. Sukhbaatar, R. Fergus, et al. Learning multiagent communication with backpropagation. In *Advances in neural information processing systems*, pages 2244–2252, 2016.
- [43] A. Tacchetti, H. F. Song, P. A. Mediano, V. Zambaldi, N. C. Rabinowitz, T. Graepel, M. Botvinick, and P. W. Battaglia. Relational forward models for multi-agent learning. *International Conference on Learning Representations (ICLR 2019)*, 2019.
- [44] A. Voelker, I. Kajić, and C. Eliasmith. Legendre memory units: Continuous-time representation in recurrent neural networks. In *Advances in Neural Information Processing Systems*, pages 15544–15553, 2019.
- [45] R. J. Williams and D. Zipser. A learning algorithm for continually running fully recurrent neural networks. *Neural computation*, 1(2):270–280, 1989.
- [46] Z. Wu, S. Pan, F. Chen, G. Long, C. Zhang, and P. S. Yu. A comprehensive survey on graph neural networks. *arXiv preprint arXiv:1901.00596*, 2019.
- [47] S. Xingjian, Z. Chen, H. Wang, D.-Y. Yeung, W.-K. Wong, and W.-c. Woo. Convolutional lstm network: A machine learning approach for precipitation nowcasting. In *Advances in neural information processing systems*, pages 802–810, 2015.
- [48] J. Yoon, D. Jarrett, and M. van der Schaar. Time-series generative adversarial networks. In *Advances in Neural Information Processing Systems*, pages 5509–5519, 2019.
- [49] Z. Zhang, P. Cui, and W. Zhu. Deep learning on graphs: A survey. *arXiv preprint arXiv:1812.04202*, 2018.
- [50] H. Zhao, J. Shi, X. Qi, X. Wang, and J. Jia. Pyramid scene parsing network. In *Proceedings of the IEEE conference on computer vision and pattern recognition*, pages 2881–2890, 2017.

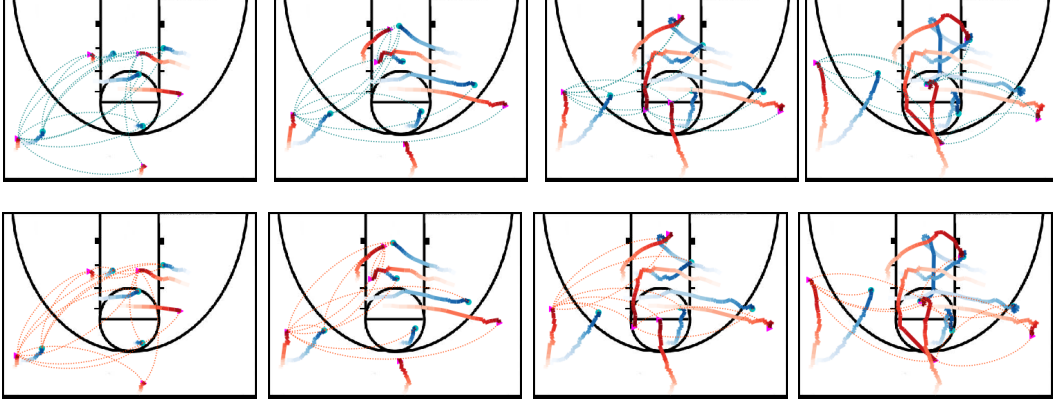


Figure 7: Visualization of the basketball players trajectories with inference period = 10. The top row visualizes the inferred interactions from the same team (coordination) and the bottom row visualizes the inferred interactions from different teams (competition). Different columns represent different time steps.

Appendix

6 Visualization of the other edge type in the Basketball Dataset

In Sec 4.2, we visualized one of the two inferred edge types. And the other edge type is visualized here. Notice that the first edge type captures focus on the rightmost red player while the second edge type captures focus on the leftmost red player.

7 Model Details

In this section, we include some details about the model implementation, especially the encoder part. Our encoder is analogical to common CNNs [17] used in the field of image recognition, where the task can be abstracted to be a classification problem on 1D dimension. Meanwhile, inspired by [50], we add additional 2 global feature extractors to combine the whole-sequence (global) features and the sub-sequence (local) features.

for DYARI-C, Each residual block shown in Fig. 3 consists of 4 skip connections structure and for DYARI-S, each residual block contains 2 skip connections.

8 Dataset Details

Particle dataset details In general, we use the same pre-processing in NRI. Each raw simulated trajectory has length of 5000 and we sample with frequency of 100 so that each sample has length of 50 in our dataset. Correspondingly, the value of dynamic period/inference period matches the length of sample in our dataset. For instance, dynamic period = 10 means that the in the raw trajectory, the state of a node changes every 1000 time steps. In addition, The value of trajectories are all normalized to range of $[0, 1]$ and the evaluation is done on the same range as well.

Basketball dataset details The basketball dataset consists of trajectory from 30 teams. The raw trajectory is captured with frequency of 25 ms. For our experiment, we sample the trajectory with frequency of 50 ms for more evident change of coordinates of players. Meanwhile, the values of the trajectories are normalized to range $[0, 1]$ as well and inference period matches the length of sample as well. For instance, inference period = 10 means that our model produce prediction every 500 ms.